

# Micromachined microbial and photosynthetic fuel cells

Mu Chiao<sup>1</sup>, Kien B Lam<sup>2</sup> and Liwei Lin<sup>2</sup>

<sup>1</sup> Department of Mechanical Engineering, The University of British Columbia, 6250 Applied Science Lane, Vancouver, BC V6T 1Z4, Canada

<sup>2</sup> Berkeley Sensor and Actuator Center, University of California at Berkeley, Berkeley, CA 94720-1740, USA

E-mail: [muchiao@mech.ubc.ca](mailto:muchiao@mech.ubc.ca)

Received 26 April 2006, in final form 26 September 2006

Published 18 October 2006

Online at [stacks.iop.org/JMM/16/2547](http://stacks.iop.org/JMM/16/2547)

## Abstract

This paper presents two types of fuel cells: a miniature microbial fuel cell ( $\mu$ MFC) and a miniature photosynthetic electrochemical cell ( $\mu$ PEC). A bulk micromachining process is used to fabricate the fuel cells, and the prototype has an active proton exchange membrane area of 1 cm<sup>2</sup>. Two different micro-organisms are used as biocatalysts in the anode:

(1) *Saccharomyces cerevisiae* (baker's yeast) is used to catalyze glucose and (2) *Phylum Cyanophyta* (blue-green algae) is used to produce electrons by a photosynthetic reaction under light. In the dark, the  $\mu$ PEC continues to generate power using the glucose produced under light. In the cathode, potassium ferricyanide is used to accept electrons and electric power is produced by the overall redox reactions. The bio-electrical responses of  $\mu$ MFCs and  $\mu$ PECs are characterized with the open-circuit potential measured at an average value of 300–500 mV. Under a 10 ohm load, the power density is measured as 2.3 nW cm<sup>-2</sup> and 0.04 nW cm<sup>-2</sup> for  $\mu$ MFCs and  $\mu$ PECs, respectively.

(Some figures in this article are in colour only in the electronic version)

## 1. Introduction

Microbial fuel cells (MFCs) have been studied extensively for more than a decade [1, 2]. A MFC uses micro-organisms as a biocatalyst to generate electricity from glucose. The electrochemistry associated with different organisms including baker's yeast [3, 4], sea floor bacteria [5], neutral red (NR) [6] and other organisms [7] has been studied in MFCs. Figure 1 shows the operation principle of a MFC. The anode and cathode reaction chambers are separated by a proton exchange membrane (PEM) and connected by electrodes through an external circuit. In the anode, a live culture of a micro-organism is suspended in a buffer solution with a carbohydrate such as glucose and with a redox coupler or electron mediator. As the microbes catabolize glucose, electrons are generated and stored in a series of intermediates such as NADH, or along the respiratory electron chain in the mitochondria [8]. Redox electron mediators in the solution diffuse into the microbial cells. The mediators are competing with oxygen to oxidize some of these electrons from their regular metabolic

activities, and diffuse back out of the microbial cell walls [9]. More detailed charge transfer mechanism can be found in previous reports [2, 4]. Ideal redox electron mediators for this application should (1) have a redox potential sufficiently positive to oxidize NADH, (2) form those redox couples reversibly enough to be able to give up the electron to the electrode, (3) be stable in both oxidized and reduced forms to endure long-term redox cycling, (4) be soluble in aqueous media near neutral or physiological pH, and (5) be able to be absorbed into or diffuse through cell or organelle membranes. By diffusion, the reduced electron mediators travel through the buffer solution and eventually deposit their electrons on the anode. There, the electrons are received by an electron acceptor (i.e. oxidant) such as ferricyanide (symbolized by Fe(III) in ), completing the circuit.

Like a MFC, a photosynthetic electrochemical cell (PEC) uses a micro-organism to generate electricity [2]. However, a PEC is powered by sub-cellular photosynthetic components. *Synechococcus* sp [10] and *anabaena variabilis* [11] have been

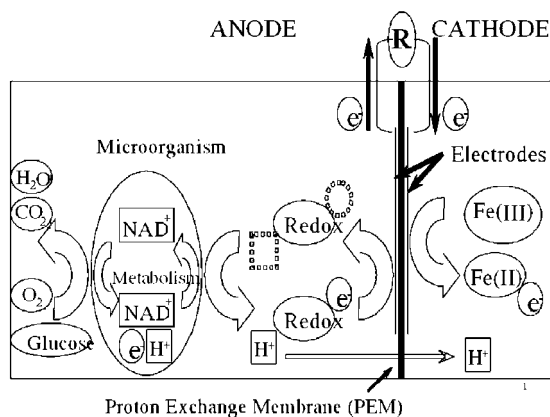


**Figure 1.** Principles of operation of a MFC. Catabolic metabolism breaks down carbohydrate substrates (such as glucose) and releases electrons from mitochondria. A redox mediator siphons these electrons (and protons,  $H^+$ ) and transports them to the anodic electrode. They then travel through an external load ( $V$ ) to the cathodic electrode, where they reduce oxidant  $Fe(III)$  to  $Fe(II)$ . Simultaneously, protons ( $H^+$ ) diffuse from the anode across the PEM into the cathode.

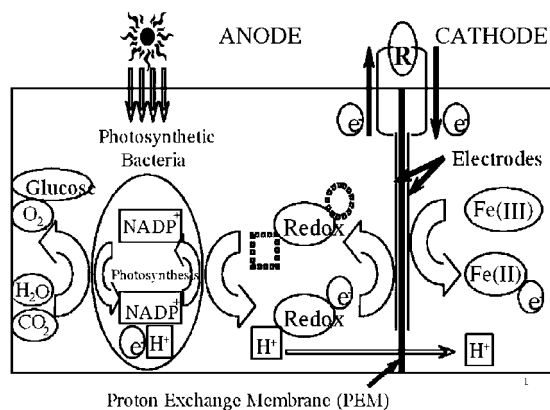


**Figure 2.** Principles of operation of a PEC. In the presence of light, during photosynthesis, electrons are transported through the photosystems in thylakoid membranes. A redox mediator siphons these electrons (and protons,  $H^+$ ) from the thylakoids and transports them to the anodic electrode. They then travel through an external load ( $V$ ) to the cathodic electrode, where they reduce oxidant  $Fe(III)$  to  $Fe(II)$ .

studied. It was understood that PECs generate electricity from both photosynthesis and catabolism of endogenous carbohydrates in the light and from catabolism alone in the dark. The implementation of a PEC is illustrated in figure 2, which shows that the anode and cathode reaction chambers are separated by a PEM and connected by electrodes through an external circuit. In the anode chamber, a live culture of photosynthetic bacteria is suspended in a solution with a redox coupler or an electron mediator. Provided with light, the photosynthetic bacterial cells carry on the reactions of photosynthesis, converting  $CO_2$  and  $H_2O$  into  $O_2$  and carbohydrates (e.g. glucose). During photosynthesis, electrons are being shuttled in the diffusional electron carriers NADPH or along a series of thylakoid-membrane-bound enzyme complexes of the electron transport chain. These electrons (and protons) are siphoned from their normal

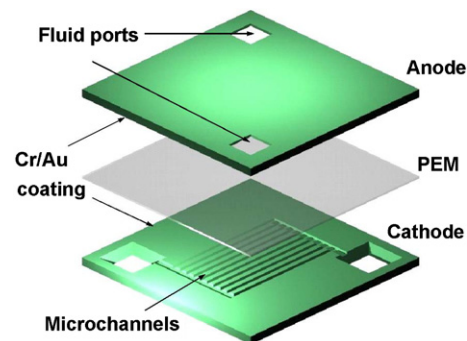


**Figure 3.** Exploded view of a  $\mu$ MFC.

photosynthetic duties either from NADPH or the transport chain by redox electron mediator molecules that have diffused into the bacterial cells. Then these reduced (electron- and proton-carrying) mediators make their way back by diffusion out of the bacterial cells, through the buffer solution, and eventually donate the electrons to the anode. Just as in the MFC, the electrons then travel through an external load into the cathode chamber, where they reduce the oxidant ferricyanide ( $Fe(III)$ ). The protons cross the PEM from the anode into the cathode, where they combine with the reduced oxidant ( $Fe(II)$ ) or with  $O_2$  and electrons from the reduced oxidant to release  $H_2O$ .

Miniaturized, portable power sources are important components for the realization of complete microsystems. Previous approaches include micro-turbine engines [12], micro-batteries [13] and micro-thermoelectric generators [14]. Micro-turbine engines have a high energy density, but the high surface area-to-volume ratio in the micro-scale makes micro-engines prone to thermal losses to the environment. A micro-battery has lower energy density than methanol fuel cells [15], but micro-batteries typically do not require fluid transfer ports and are easier to construct than fuel cells from the micromachining point of view. Micro-thermoelectric generators require a temperature difference that is difficult to maintain in the micro-scale. The efficiency of thermoelectric conversion is also lower than combustion due to limitations in the available thermoelectric material.

In the area of miniaturized fuel cells, methanol has been demonstrated as the fuel to generate electricity [16, 17]. However, the technical limitations of the materials (both the catalysts and the membranes) used in methanol fuel cells may reduce the practical advantages in terms of performance and cost over batteries [15]. Micromachined microbial fuel cells ( $\mu$ MFCs and  $\mu$ PECs) were first reported by our group. Current density of a  $\mu$ MFC was characterized for 14 min under a 10 ohm load [18]. Two trial tests for algae cultured under 2 and 4 days were recorded in the  $\mu$ PEC experiments [19]. In this paper, an extended testing period and more experiments are reported.

## 2. Design and fabrication

To implement the  $\mu$ MFC and  $\mu$ PEC concepts, we designed a MEMS-based fuel cell consisting of stacked Si and/or glass substrates. The exploded view of a  $\mu$ MFC is shown in figure 3.

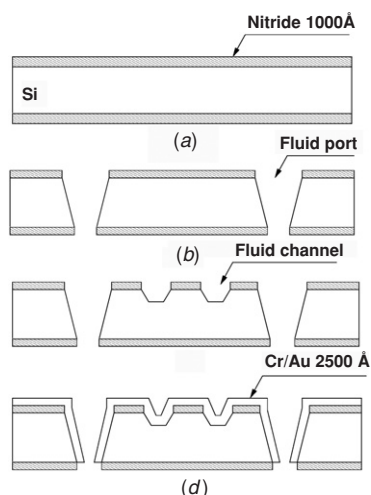


**Figure 4.** Fabrication processes of the  $\mu$ MFC.

Two factors affect the design considerations of the microbial fuel cell: (1) the biocatalytic reaction should take place at the immediate vicinity of the PEM such that the proton traveling distance can be minimized and the energy transfer efficiency can be optimized and (2) the surface area-to-volume ratio of the anode and cathode compartments should be maximized to achieve high energy density as well as high coulombic yield. Micromachined fluid channels are designed to form in the anode and cathode compartments to achieve a high surface-to-volume ratio and grant the biocatalyst and fuel access to the PEM. The microchannel surfaces are coated with Cr/Au as the current collectors. A Dupont Nafion-117<sup>TM</sup> film is used as the PEM and is sandwiched between the anode and the cathode. The size of the microchannel is designed such that it allows the micro-organisms to flow through and clogging can be avoided. Typically, the size of a yeast cell is about 10  $\mu\text{m}$  in diameter. Therefore, microchannels with sizes of 100  $\mu\text{m}$  wide and 80  $\mu\text{m}$  deep are designed.

The fabrication processes are shown in figure 4. A p-type silicon wafer is deposited with LPCVD low stress nitride of 1000 Å in thickness as a hard mask (figure 4(a)). The first photolithography step is used to define the fluid ports. The anisotropic etchant, KOH:H<sub>2</sub>O = 1:2 by weight at 80 °C, is used to etch through the silicon wafer (figure 4(b)). The second photolithography step is then used to define the fluid channel (figure 4(c)). In this step, thick spin-on photoresist (thickness  $\sim$ 9  $\mu\text{m}$ ) is used to overcome surface roughness which resulted from the first KOH etch. Timed etch in the KOH etchant is then used to make 80  $\mu\text{m}$  deep fluid channels. After the fluid ports and channels are formed on the silicon wafer, Cr/Au of 2500 Å thick is thermally evaporated on to the silicon microchannel as the current collector (figure 4(d)). Cr of 200 Å acts as an adhesion layer. The slanted channel wall enables a conformal deposition of Cr/Au and makes the electrical connection to the external world possible.

Figure 5 shows the SEM microphoto of the fabrication result of the fluid port and channels. The area of the fluid port is 1000  $\times$  1000  $\mu\text{m}^2$  and the channel width and length are 100  $\mu\text{m}$  and 6200  $\mu\text{m}$ , respectively. The total electrode area is 0.51  $\text{cm}^2$  and the surface area-to-volume ratio is about

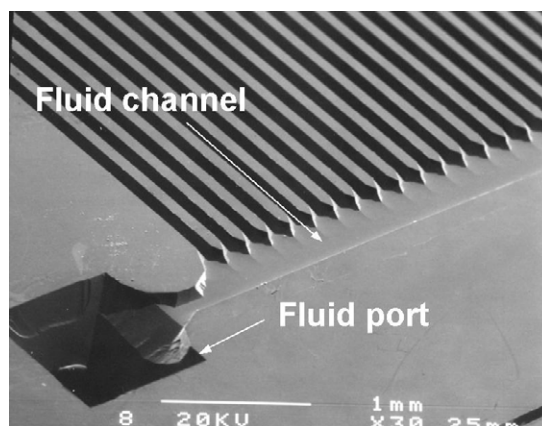


**Figure 5.** SEM microphoto shows the fluid port and channels of a  $\mu$ MFC.

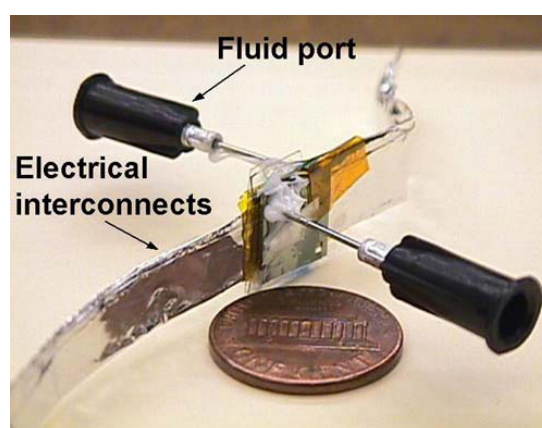


**Figure 6.** A  $\mu$ MFC after final assembly.

500  $\text{cm}^{-1}$  (the surface area-to-volume ratio with a plain electrode surface is only about 120  $\text{cm}^{-1}$  in this case).

PEM is prepared by boiling in a solution (H<sub>2</sub>O<sub>2</sub>:H<sub>2</sub>O = 1:9 by volume) for 1 h. The PEM is then cleaned in boiling DI water for 2 h. This procedure is then repeated for one more time. The cleaning procedure would remove metallic and organic contaminations on the PEM surface [17]. Care must be taken when handling the PEM after it has been cleaned to maintain its proton-conducting capability. The PEM is then glued to the silicon substrates at the edges using silicone. The electrical connection to the outside world is made by attaching aluminum foil to the Cr/Au surface. The final assembly is shown in figure 6.

The  $\mu$ PEC fabrication process is similar to  $\mu$ MFCs. However, a  $\mu$ PEC needs to have a transparent cover that permits light to enter the chamber. The exploded view of a  $\mu$ PEC is shown in figure 7. The final physical size of a  $\mu$ PEC is 1.5  $\text{cm} \times$  1.5  $\text{cm} \times$  2.5  $\text{mm}$ . To facilitate the injection of the reaction mixtures into the chambers, fluid ports (800  $\mu\text{m} \times$  5  $\text{mm}$ ) were etched in the Si substrate. Smaller through-holes (280  $\mu\text{m} \times$  280  $\mu\text{m}$ ) were etched in the reaction chamber, permitting the reaction mixture to contact the gold film deposited on the surface opposite the chamber and the proton-exchange membrane. Finally, a PEM is compressed between the two reaction chambers.

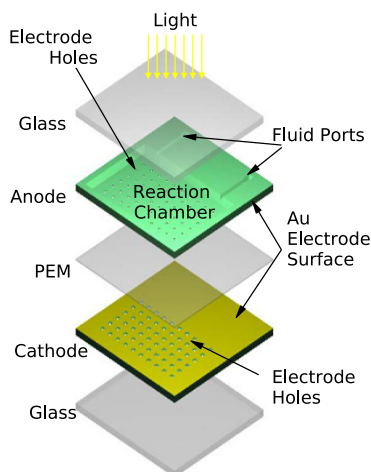


**Figure 7.** Exploded view of a  $\mu$ PEC. The glass cap permits light to enter the chamber for the  $\mu$ PEC. The electrode holes allow the reaction mixtures to contact the gold electrode surface.

### 3. Experimental procedures and results

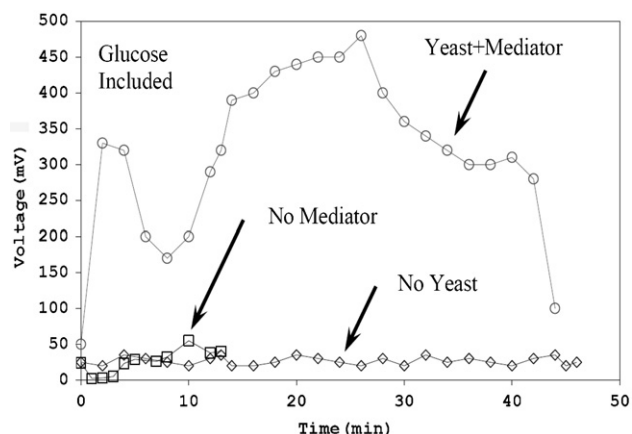
#### 3.1. $\mu$ MFCs

The culturing of *Saccharomyces cerevisiae* follows the biology laboratory protocol [20]. The nutrient suitable for yeast to grow is prepared by mixing agar powders with glucose, yeast extracts and dissolved in distilled water. The agar nutrient is then put into an autoclave chamber for 1 h. The high temperature (120 °C) environment in the autoclave chamber is sufficient to kill unwanted bacteria species pre-existing in the nutrient mixture and prevent them from killing the yeast in the later culturing stage. After autoclaving, the nutrient becomes a liquid form and it must be poured into petri dishes before it is solidified around 42 °C. The nutrient petri dishes can be stored in the refrigerator before use. The mother strain *Saccharomyces cerevisiae* is purchased from a biological supply company<sup>3</sup> and is kept in the refrigerator before use. Once the nutrient petri dish is prepared, the strain of *Saccharomyces cerevisiae* is physically rubbed off from the mother plate by a sterile platinum loop and streak on to the nutrient petri dish. The petri dish is then covered and incubated under room temperature for 48 h.

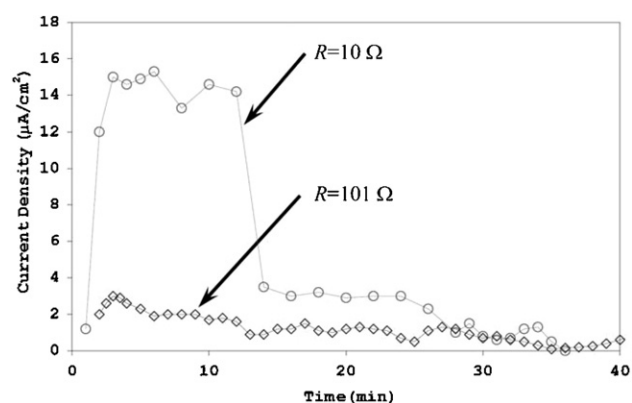
The anolyte and catholyte are prepared subsequently. For anolyte, micro-organism culture is mixed with 1 M of glucose in a 0.1 M phosphate buffer (pH 7.0). The electron transfer mediator, methylene blue of 0.01 M is then added. On the cathode side, a 0.02 M potassium ferricyanide solution is prepared in a 0.1 M phosphate buffer (pH 7.0). The bio-electrical responses are measured by dropping a drop of each corresponding solutions into the anode and cathode compartments, and the electrical signals are measured chronically.

Figure 8 shows that the  $\mu$ MFC produces an OCV only when the three critical elements were present in the anode reaction mixture: (1) biocatalyst (i.e. bakers yeast), (2) bio-fuel (i.e. glucose) and (3) redox mediator (i.e. methylene blue). When neither mediator nor yeast was presented, the  $\mu$ MFC

<sup>3</sup> Sigma-Aldrich Corporate Offices, 3050 Spruce St, St. Louis, MO 63103, USA.



**Figure 8.** OCV measurement of a  $\mu$ MFC with glucose. Without the yeast or without the redox mediator in the anode reaction mixture, negligible OCV is produced.



**Figure 9.** Current density measurement of a  $\mu$ MFC under two resistive loads.

generated negligible OCV, but when all three elements were presented, the  $\mu$ MFC generated a peak voltage of over 450 mV and sustained over 300 mV for over 20 min (over 250 mV for over 30 min). The rapid drop-off of output at 40 min was due to the drying out by evaporation of the small (16  $\mu$ L) anode and cathode reaction chambers, which were manually injected by a syringe into the chambers at the start of the experiment and were not refilled. Because of evaporation and occasionally incomplete filling of the chambers by manual injection (due to air bubbles), the duration of electrical output by the  $\mu$ MFC varied from experiment to experiment, ranging from about 20 min to an hour. In addition, the mass of yeast used in each run was not well controlled or documented, resulting in variations and lack of repeatability in the output.

The measured current under two resistive loads:  $R = 10$  ohm and 101 ohm has been normalized by the area of the PEM (1  $\text{cm}^2$ ). As shown in figure 9, under the 10 ohm load, the  $\mu$ MFC produced a peak current of 15  $\mu\text{A cm}^{-2}$  and a corresponding power density of 2.3  $\text{nW cm}^{-2}$ . After sustaining over 13  $\mu\text{A cm}^{-2}$  for about 10 min, the current drastically dropped to about 3  $\mu\text{A cm}^{-2}$  and remained at that level for another 10 min before gradually declining to zero, which again corresponded to the anode reaction mixture having completely evaporated. It was occasionally observed that quick de-wetting occurs in the reaction chamber. In such a

case, less of the reaction mixture would make contact with the Au electrode surface and PEM with reduced electrical output as a result. When the evaporation did not produce fast de-wetting of the solution from the chamber, the current density curve did not exhibit drastic changes, such as the one for  $R = 101$  ohm in figure 9, which peaked at about  $3 \mu\text{A cm}^{-2}$  and very gradually declined to zero.

The coulombic yield efficiency of the MFC can be calculated. The complete catabolism of 1 M of glucose ( $\text{C}_6\text{H}_{12}\text{O}_6$ ) yields 6 M of  $\text{CO}_2$ , 6 M of  $\text{H}_2\text{O}$  and 32 M of ATP. What is not shown in the equation was that during the process of catabolism, electrons are generated and transported in the form of electron carriers such as NADH. In fact, the catabolism of 1 molecule of glucose generates 24 electrons (and 24 protons,  $\text{H}^+$ ). Knowing this, we can calculate the number of electrons (in the form of coulombs) theoretically available from the 1 M glucose in the  $16 \mu\text{L}$  anode chamber:

$$16 \times 10^{-6} \text{L} \times \frac{1 \text{mole glucose}}{L} \times 6.023 \times 10^{23} \frac{\text{molecules}}{1 \text{mole glucose}} \times 24 \frac{\text{electrons}}{1 \text{mole glucose}} \times 1.6 \times 10^{-19} \frac{\text{C}}{\text{electron}} = 37 \text{C}. \quad (1)$$

We then estimate the number of coulombs generated by the  $\mu\text{MFC}$  by integrating the area under the  $R = 10$  ohm curve in figure 9. We approximate the curve as being composed of three rectangles, one of height  $13 \mu\text{A cm}^{-2}$  for about 10 min, another one of height  $3 \mu\text{A cm}^{-2}$  for another 10 min and a third of height  $1 \mu\text{A cm}^{-2}$  for another 10 min. Noting that Ampere = Coulomb  $\text{s}^{-1}$  and using the  $1 \text{ cm}^2$  nominal area of the  $\mu\text{MFC}$ , we find that the number of coulombs recovered from the supplied glucose by the  $\mu\text{MFC}$  is

$$(13 \times 10^{-6} \text{C s}^{-1} + 3 \times 10^{-6} \text{C s}^{-1} + 1 \times 10^{-6} \text{C s}^{-1}) \times 10 \text{ min} \times 60 \text{ s min}^{-1} = 0.01 \text{C}. \quad (2)$$

Comparing equations (1) and (2), we find that the  $\mu\text{MFC}$  coulombic efficiency was

$$\frac{0.01\text{C}}{37\text{C}} = 0.027\% \quad (3)$$

that is significantly lower than the roughly 40% coulombic efficiency reported [3].

### 3.2. $\mu\text{PECs}$

*Phylum Cyanophyta* commonly known as blue-green algae, the unicellular *Anabaena* is one of the simplest photosynthetic bacteria that have the complete photosynthetic Z-Scheme. Cultures of *Anabaena* sp. in an Alga-Gro Freshwater medium (pH 7.8) were purchased<sup>4</sup> and were kept under illumination until the experiments. The anolyte for the experiments was prepared using samples of *Anabaena* in its Alga-Gro medium and 0.01 M methylene blue as the electron mediator. Glucose was not added at this stage and Alga-Gro itself contains no glucose or complex nutrient molecules like carbohydrates. The catholyte consisted of 0.02 M potassium ferricyanide as the electron acceptor (oxidant) in a 0.1 M sodium phosphate buffer (pH 7). Using methylene blue as the redox mediator in the anode and ferricyanide as the oxidant in the cathode, the

<sup>4</sup> Carolina Biological Supply Company, 2700 York Road, Burlington, NC 27215-3398, USA.

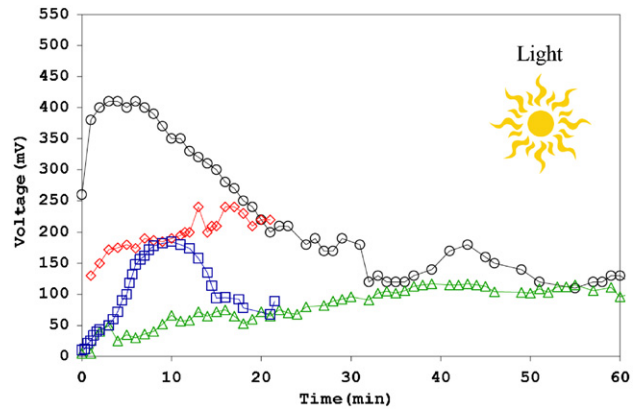


**Figure 10.** OCV measurement of a  $\mu\text{PEC}$  with four representative trials carried out under light. Algae cultured between 2 days ( $\circ$ ) and 4 days ( $\square$ ) were tested. Higher OCV achieved by the 2 day culture was due to higher metabolic activities of the algae in an initial growth phase.

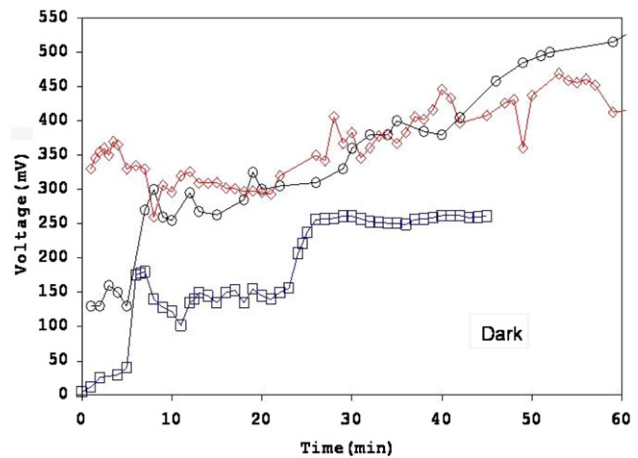


**Figure 11.** OCV measurement of a  $\mu\text{PEC}$  with three representative trials carried out in the dark.

overall chemical equation of the  $\mu\text{PEC}$  is the same as that for the  $\mu\text{MFC}$ .

A desk lamp with a 60 W light bulb was used as the light source. In the light experiments, the  $\mu\text{PEC}$  was positioned about 12 inches from the desk lamp light bulb. In this case, the electrical output being generated by the  $\mu\text{PEC}$  was due mostly to the photosynthetic light reactions. In the dark (no-light) experiments, the  $\mu\text{PEC}$  was wrapped in an Al foil to shield it from light. The reaction mixtures were manually dispensed from syringes directly into the  $\mu\text{PEC}$  via its fluid delivery ports until the reaction chambers were as full as possible (about  $16 \mu\text{L}$  when completely full).

Under the illumination of a 60 W desk lamp, the  $\mu\text{PEC}$  generated electrical output, as much as 400 mV peak OCV and over 200 mV sustained for 20 min, as shown in figure 10. After 20 min, the output gradually decreased to around 100 mV past 60 min. However, in other trials, the peak levels were often lower and the output duration shorter again, most likely due to the incomplete filling of the reaction chambers or the evaporation of the reaction mixture. Previous studies suggested that a PEC functions like a MFC in the dark [10]. This was also observed in the  $\mu\text{PEC}$ . In figure 11, catabolic

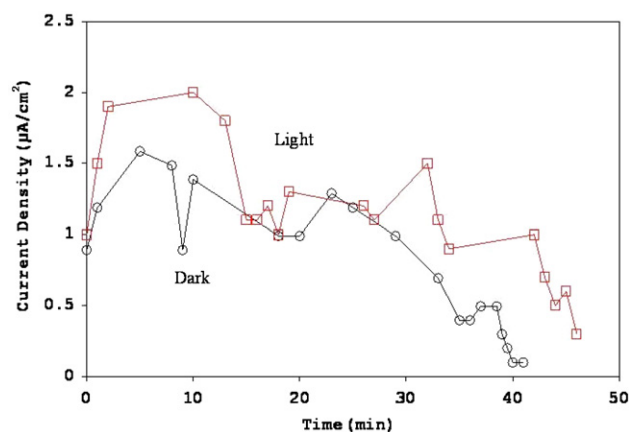


**Figure 12.** Current density of  $\mu$ PEC with load  $R = 10$  ohm was comparable in the light and dark.

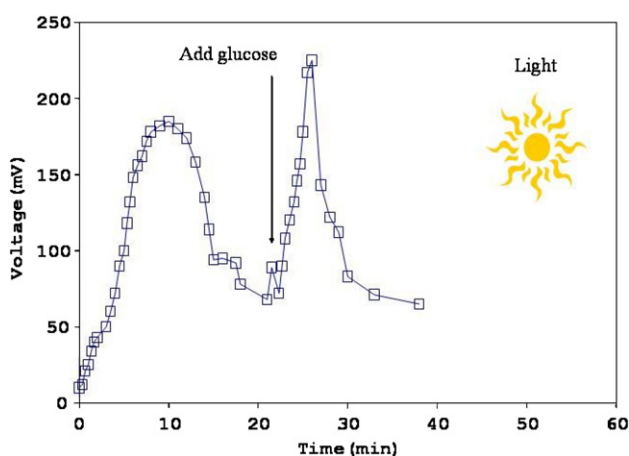


**Figure 13.** The  $\mu$ PEC in light was rejuvenated in terms of OCV when an external dose of glucose was added.

metabolism persists in the  $\mu$ PEC in the dark, consuming complex nutrient molecules such as glucose that they produced internally when light was present. In the dark, the  $\mu$ PEC yielded as much as 500 mV OCV, an output level that was actually sustained past an hour. Based on these trials, it might even seem that the duration of the electrical output in the dark was longer than in the light. We suspected that, without the heat of the 60 W bulb nearby, evaporation of the reaction mixtures occurred more slowly. Figure 12 shows the current measurement. Both the light and dark curves had peak current densities of 1.5 to  $2 \mu\text{A cm}^{-2}$  and corresponding power densities of 0.02 to  $0.04 \text{ nW cm}^{-2}$ . Conservatively, estimating an illumination intensity of  $1 \text{ mW cm}^{-1}$ , we can calculate that the light conversion efficiency of the  $\mu$ PEC was much less than 1%.

Finally, to demonstrate that the  $\mu$ PEC was indeed able to run in a glucose-enabled metabolism  $\mu$ MFC mode, the  $\mu$ PEC was first operated in the light as normal. As shown in figure 13, the OCV began to decline around 20 min, and a dose of 1 M glucose was manually injected by a syringe into the anode chamber. The  $\mu$ PEC responded immediately to the infusion of fuel with a spike in OCV. This is not likely due to the rewetting of the electrode surface, as some samples were still wet when they were exhausted and reinjected with fresh

fuel. More experiments are needed to further characterize the phenomenon. The  $\mu$ PEC thus had dual modes of operation: a photosynthetic mode when light is present and a catabolic MFC mode without light. In this way,  $\mu$ PECs are more versatile than  $\mu$ MFCs.

#### 4. Conclusion and discussion

In this paper, bulk silicon micromachining technology was used to fabricate the anode and cathode compartments for  $\mu$ MFCs and  $\mu$ PECs. A  $\mu$ MFC uses *Saccharomyces cerevisiae* to catalyze glucose and generate electricity. The power density is characterized as  $2.3 \text{ nW cm}^{-2}$  and the open-circuit potential is measured as 300–400 mV. The reported yeast-based macroscale microbial fuel can reach  $2 \mu\text{W cm}^{-2}$  [21]. Furthermore, the energy conversion efficiency of the  $\mu$ MFC was estimated as 0.027% that is significantly lower than the 40% coulombic efficiency reported [3]. This low power density and low energy conversion efficiency could result from (1) oxygen in the anode compartment could strip electrons from methylene blue and reduce the total electrons transported to the anode [22] and (2) the aluminum foil and Cr/Au interface could have a high contact resistance if the gluing process is not carried out well.

A  $\mu$ PEC uses blue-green algae to generate electricity under light; when light is turned off, the  $\mu$ PEC functions like a  $\mu$ MFC. The  $\mu$ PEC has a power density of 0.02– $0.04 \text{ nW cm}^{-2}$  both in the light and in the dark. However, the energy conversion efficiency was much less than 1%. It was reported that a PEC has an efficiency of 0.2% to 3.3% [10, 23]. The presence of  $\text{O}_2$  in the anode was suppressed to minimize the oxidation of the electron-carrying redox mediator, and maximize the chance of electrons to reach the electrode. In our  $\mu$ PEC experiments, no attempt was made to suppress  $\text{O}_2$  in the anode and we conjecture that competition by  $\text{O}_2$  with the mediator for electrons in the anode decreased the overall electrical output and efficiency.

To prevent oxygen from competing with electron mediators, the anode of most macroscale MFCs and PECs are controlled under anaerobic conditions [2]. For yeast-based fuel cells, under anaerobic conditions, glucose is metabolized into alcohol and water, while electrons are still produced as under aerobic conditions [22, 24, 25]. For  $\mu$ MFCs and  $\mu$ PECs, Ar gas can be purged into the anode to minimize the oxygen level; however, this can be a challenge in a real fuel cell, as bulky gas cylinders may need to accompany the small device.

The  $\mu$ MFCs and  $\mu$ PECs may find applications in powering electronic and MEMS devices. Although the power density reported in this work is low and cannot find practical applications, with the advances in biochemistry and microbial fuel cell field, researchers can one day optimize microbial chemistry that could be used in  $\mu$ MFCs and  $\mu$ PECs. Challenges remain for MEMS researchers to build small-scale anode and cathode chambers that are suitable for specific micro-organism/mediator combination. The stand alone miniature fuel cell should minimize oxygen intake while allow waste such as  $\text{CO}_2$  to diffuse out.

## Acknowledgments

These devices are fabricated at the University of California at Berkeley Microfabrication Laboratory. This work is supported in part by a DARPA DSO/BioFlips grant (F30602-98-2-0227). M Chiao is supported by the Canada Research Chairs, Tier 2 Program.

## References

- [1] Katz E, Shipway A N and Willner I 1989 *Biochemical Fuel Cells Handbook of Fuel Cells—Fundamentals, Technology and Applications* 355–381 (Materials Park, OH: ASM International)
- [2] Bullen R A, Arnot T C, Lakemanc J B and Walsh F C 2006 Biofuel cells and their development *Biosens. Bioelectron.* **21** 2015–45
- [3] Bennetto H P 1990 Electricity generation by microorganisms *Biotechnol. Educ.* **1** 163–9
- [4] Delaney G M, Bennetto H P, Mason J R, Roller S D, Stirling J L and Thurston C F 1984 Electron-transfer coupling in microbial fuel cells: II. Performance of fuel cells containing selected microorganism-mediator-substrate combinations *J. Chem. Tech. Biotechnol.* **34B** 13–27
- [5] Halme A, Zhang X and Ranta A 2000 Study of biological fuel cells *Proc. 2nd Annual Advances in R&D: The Commercialization of Small Fuel Cells and Battery Technologies for Use in Portable Applications*
- [6] Park D H and Zeikus J G 2000 Electricity generation in microbial fuel cells using neutral red as an electronophore *Appl. Environ. Microbiol.* **66** 1292–7
- [7] Chaudhuri S K and Lovley D R 2003 Electricity generation by direct oxidation of glucose in mediatorless microbial fuel cells *Nature Biotechnol.* **21** 1229–32
- [8] Bennetto H P, Stirling J L and Tanaka K 1985 Reduction of redox mediators by NADH electron transduction in bioelectro-chemical systems *Chem. Ind.* **b** 695–7
- [9] Roller S D, Bennetto H P, Delaney G M, Mason J R, Stirling J L and Thurston C F 1984 Electron-transfer coupling in microbial fuel cells: I. Comparison of redox mediator reduction rates and respiratory rates of bacteria *J. Chem. Tech. Biotechnol.* **34B** 3–12
- [10] Yagishita T, Horigome T and Tanaka K 1993 Effects of light, CO<sub>2</sub>, and inhibitors on the current output of biofuel cells containing the photosynthetic organism *Synechococcus* sp *J. Chem. Tech. Biotechnol.* **56** 393–9
- [11] Tanaka K, Kashiwagi N and Ogawa T 1988 effects of light on the electrical output of bioelectrochemical fuel-cells containing *Anabaena variabilis* m-2 mechanisms of the post-illumination burst *J. Chem. Tech. Biotechnol.* **42** 235–40
- [12] Mehra A, Zhang X, Ayon A A, Waitz I A, Schmidt M A and Spadaccini C M 2000 Six-wafer combustion system for a silicon micro gas turbine engine *J. Microelectromech. Syst.* **9** 517–27
- [13] Lee K B and Lin L 2002 Electrolyte based on-demand and disposable microbattery *Tech. Dig. IEEE Micro Electro Mechanical Systems (Jan. 2002)* pp 236–9
- [14] Toriyama T, Yajima M and Sugiyama S 2001 Thermoelectric micro power generator utilizing self-standing polysilicon-metal thermopile *Tech. Dig. MEMS 2001: 14th IEEE Int. Conf. on Micro Electro Mechanical Systems (Jan. 2001)* pp 562–5
- [15] Dyer C K 2002 Fuel cells for portable applications *J. Power Source* **106** 31–4
- [16] Kelley S C, Deluga G A and Smyrl W H 2002 Miniature fuel cells fabricated on silicon substrates *AIChE J.* **48** 1071–82
- [17] Sim W Y, Kim G Y and Yang S S 2001 Fabrication of micro power source(mps) using micro direct methanol fuel cell for the medical application *Tech. Dig. IEEE MEMS Conf. (Jan. 2001)* pp 341–4
- [18] Chiao M, Lam K B and Lin L 2003 Micromachined microbial fuel cells *Proc. IEEE Micro Electro Mechanical Systems (MEMS) (Jan. 2003)* pp 383–6
- [19] Lam K B, Chiao M and Lin L 2003 A micro photosynthetic electrochemical cell *Proc. IEEE Micro Electro Mechanical Systems (MEMS) (Jan. 2003)* pp 391–4
- [20] Davis J M 1994 *Basic Cell Culture: A Practical Approach* (Oxford: IRL Press)
- [21] Bennetto H P, Stirling J L, Tanaka K and Vega C A 1983 Anodic reactions in microbial fuel cells *Biotechnol. Bioeng.* **25** 559–68
- [22] Thruston C F, Bennetto H P, Delaney G M, Mason J R, Roller S D and Stirling J L 1985 Glucose metabolism in a microbial fuel cell stoichiometry of product formation in a thionine-mediated proteus-vulgaris fuel cell and its relation to coulombic yields *J. Gen. Microbiol.* **83** 1393–402
- [23] Yagishita T, Sawayama S, Tsukahara K T and Ogi T 1998 Performance of photosynthetic electrochemical cells using immobilized *Anabaena variabilis*-3 in discharge/culture cycles *J. Ferment. Bioeng.* **85** 56–549
- [24] Aidela H A and Arvia A J 1975 The response of a bioelectrochemical cell with *Sacharomyces cerevisiae* metabolizing glucose under various fermentation conditions *Biotechnol. Bioeng.* **27** 1529–43
- [25] Bennetto H P and Stirling J L 1983 Anodic reaction in microbial fuel cell *Biotechnol. Bioeng.* **25** 559–68